Pergamon

Available online at www.sciencedirect.com
SCIENCE DIRECT®

Cement and Concrete Research 33 (2003) 1623–1630

CEMENT AND CONCRETE RESEARCH

A comparative study of ordinary and mineralised Portland cement clinker from two different production units Part II: Characteristics of the calcium silicates

Anna Emanuelson[a], Angel R. Landa-Cánovas[b], Staffan Hansen[a,*]

[a]*Department of Materials Chemistry, Center for Chemistry and Chemical Engineering, Lund University, P.O. Box 124, SE-221 00 Lund, Sweden*
[b]*Centro de Microscopía Electrónica, Universidad Complutense de Madrid, ES-280 40 Madrid, Spain*

Received 21 November 2002; accepted 21 March 2003

Abstract

Portland cement clinkers from two production units were investigated in order to determine the effects of mineralisation on alite and belite; Plant 1: ordinary clinker (P1) and clinker mineralised with $CaF_2 + CaSO_4$ (P1m); Plant 2: ordinary clinker (P2) and two clinkers mineralised with $CaF_2 + CaSO_4$ (P2m, P2m′).

The polymorphism of alite was studied using synchrotron X-ray powder diffraction (XRD), wavelength 1.5227 Å, and electron diffraction (ED) in a transmission electron microscope. The substitutions of minor elements in alite and belite were determined using electron microprobe analysis. Clinkers P1 and P1m both contained apparent rhombohedral alite (XRD) with an incommensurately modulated structure (ED), while clinkers P2, P2m, and P2m′ all contained monoclinic alite (XRD). The addition of mineralisers in the process caused increased content of fluoride in alite and increased substitution of Si(4+) by Al(3+) and S(6+) in both calcium silicates. The latter effect was most pronounced in clinker P1m due to its high molar SO_3 to alkali oxide ratio ($R = 2.18$).

The improved hydraulic activity of P1m compared to P1 was caused by substitutions rather than a change in symmetry. The decreased hydraulic activity of P2m and P2m′ compared to P2 was explained by the high levels of fluorine, which had a retarding effect on the hydration.

Keywords: TEM; X-ray diffraction; Ca_2SiO_4; Ca_3SiO_5; Microprobe analysis

1. Introduction

The material used in this investigation includes five clinkers from two different production units, Plant 1 and Plant 2 (see Ref. [1]). The raw mix in Plant 1 consists mainly of fine-grained chalk and fly ash and the clinker is produced in a precalciner process. The compositions of the clinkers are typically in the region of ordinary Portland clinker [2]. Plant 2 uses a dry process and the raw mix consists mainly of crystalline limestone and blast furnace slag. The clinkers have a higher level of minor elements, in particular fluoride, magnesium (present partly as periclase), and alkali, and they are richer than the corresponding clinkers from Plant 1 in free lime and sulfate phases. Plant 1 has supplied one ordinary Portland clinker and one clinker mineralised with calcium fluoride and calcium sulfate. Plant 2 has supplied one ordinary Portland clinker and two clinkers mineralised with calcium fluoride and different amounts of calcium sulfate. A cement based on the Plant 1-mineralised clinker reacts more slowly during the early hydration than corresponding ordinary clinker, but then accelerates to reach higher reaction rate after 12 h. The cements based on the Plant 2-mineralised clinkers react more slowly than the corresponding ordinary cement [1].

The modified hydraulic activity of a mineralised clinker can be due to a change in the quantitative phase composition of the clinker (see Ref. [1]), or it can be caused by the modified reactivity of the separate clinker phases. In an extensive review of the subject, Moir and Glasser [3] have suggested three mechanisms that can affect the hydraulic activity of the clinker phases in a mineralised clinker: (i) reactive high temperature polymorphs can be stabilised at ambient temperature, (ii) defects can be introduced by substitutions and solid solutions, and (iii) other effects can

* Corresponding author. Tel.: +46-46-222-8117.
E-mail address: staffan.hansen@materialkemi.lth.se (S. Hansen).

0008-8846/03/$ – see front matter © 2003 Elsevier Ltd. All rights reserved.
doi:10.1016/S0008-8846(03)00114-5

arise during the hydration process, e.g., coating of particles by insoluble salts.

The aim of the present work was to outline the effects of calcium sulfate and calcium fluoride mineralisation on the calcium silicates, alite, and belite in clinkers from the two production units, and thereby explain any differences in hydraulic activity of the clinkers.

2. Experimental

Ground clinker was packed in a glass capillary (Glas, 0.30-mm outer diameter). Synchrotron X-ray powder diffraction (XRD) spectra were recorded using a Huber image foil camera 670, covering $2\theta = 8-100°$. Each diffraction pattern was collected for 10 min on beam line I711 at MAX-lab in Lund and the X-ray wavelength was 1.5227 Å. The X-ray diffraction data was used to study the alite peak at $2\theta \approx 50-51°$.

Crushed and ground clinker was dispersed on copper grids covered with holey carbon film and examined by electron diffraction (ED) techniques using a JEM-2000FX transmission electron microscope, operated at 200 kV.

Clinker grains were embedded in a low viscosity epoxy resin under vacuum, ground planar with SiC and polished with diamond powder. A thin layer of carbon was evaporated onto the sample. Quantitative microanalysis was performed at Uppsala University using a CAMECA SX50 electron microprobe. The analyses were made at an acceleration voltage of 20 kV, with a probe current of 25 nA and 1–2 μm spot size. One microprobe analysis was performed per alite or belite grain and 7–19 grains were analysed in each sample.

Table 1
Average microprobe analysis of alite, estimated S.D. (in parenthesis) referring to the last digit

Molar content	Plant 1		Plant 2		
	Ordinary	Mineralised	Ordinary	Mineralised (low SO_3)	Mineralised (high SO_3)
Ca	2.84(3)	2.85(2)	2.80(2)	2.89(2)	2.84(3)
Si	0.96(1)	0.94(2)	0.98(1)	0.95(1)	0.95(1)
Al	0.057(8)	0.08(1)	0.050(8)	0.063(6)	0.067(5)
Fe (3+)	0.028(4)	0.025(4)	0.016(3)	0.016(2)	0.015(2)
Mg	0.029(2)	0.033(3)	0.08(1)	0.061(7)	0.05(1)
S (6+)	0.004(1)	0.009(4)	0.002(1)	0.003(1)	0.006(3)
Ti	0.003(1)	0.005(1)	0.004(1)	0.002(1)	0.002(1)
P	0.02(1)	0.01(1)	0.02(2)	0.004(6)	0.01(2)
Na	0.08(5)	0.01(1)	0.019(6)	0.030(1)	0.04(2)
K	0.002(2)	0.004(2)	0.003(1)	0.003(2)	0.005(2)
O	5	5	5	5	5
No. of analyses	11	10	10	10	7

3. Results and discussion

According to the first mechanism suggested by Moir and Glasser [3], the stabilisation of a reactive high temperature polymorph can explain the modified hydraulic activity of a mineralised clinker. Clinker alite exists in three crystal systems; triclinic, monoclinic, and rhombohedral. The polymorphic state is reflected in the diffraction peak at $2\theta \approx 51-52°$ ($CuK_{\alpha 1}$ radiation). The 2θ values in our investigation are somewhat lower due to the shorter wavelength of the synchrotron beam (~ 1.52 Å) compared to $CuK_{\alpha 1}$ radiation normally used (~ 1.54 Å). Triclinic alite gives a triple peak [4], monoclinic alite gives a double peak [5], and rhombohedral alite gives a single peak [6]. After cooling, a clinker produced under normal conditions generally contains monoclinic alite [2], but it has been reported that the rhombohedral high temperature form of alite is stabilised at ambient temperature in mineralised clinker [7–10]. Other investigators have argued that this rhombohedral alite is a misinterpretation of monoclinic alite [5,11]. Substitutions may change the lattice parameters so that the double peak of monoclinic alite coalesces and the structure will be mistaken for rhombohedral [11]. The polymorphic state of belite, obtained at ambient temperature after cooling, is normally not affected by the mineralisation or substitutions [2] and is present in the monoclinic β-form in all five investigated clinkers [1].

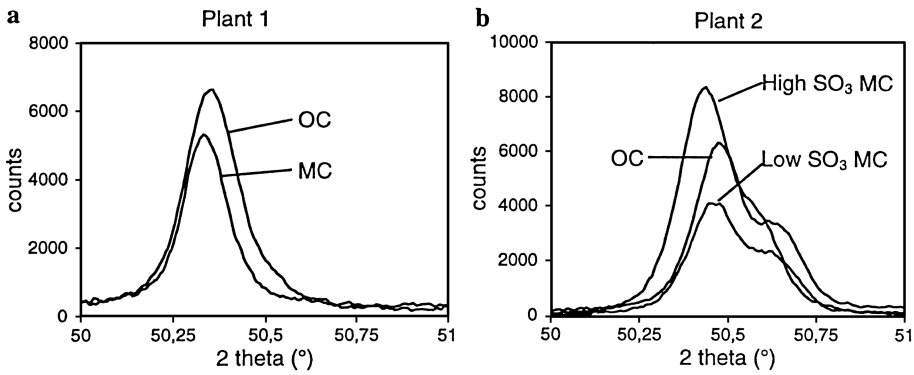

Fig. 1. Characteristic alite peaks in synchrotron XRD patterns recorded using ordinary Portland clinkers (OC) and mineralised clinkers (MC) from (a) Plant 1 and (b) Plant 2.

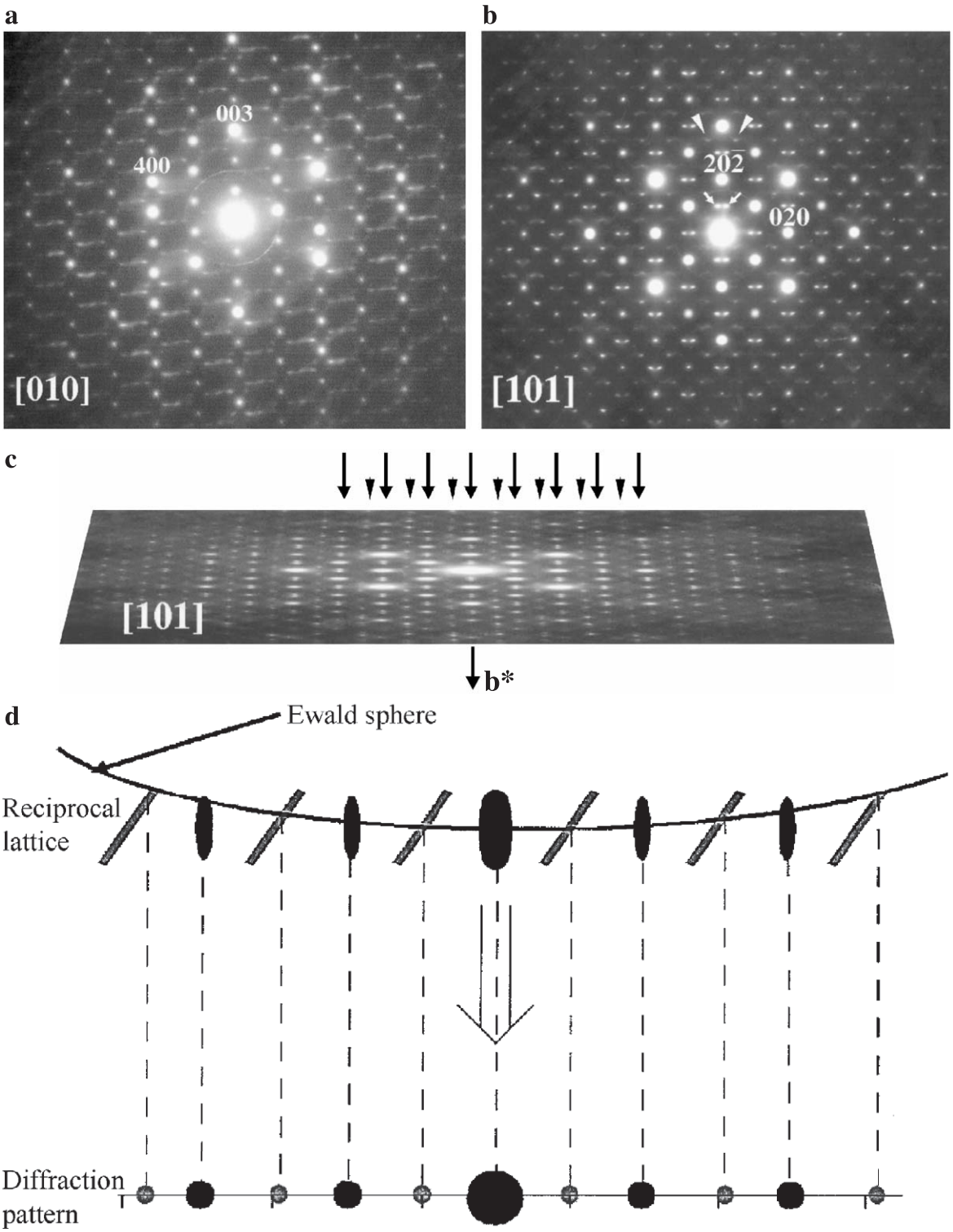

Fig. 2. (a) SAED pattern from an alite crystal along the [010] zone axis. Note the diffuse intensity rods running almost parallel to the [20-1]* direction. (b) SAED pattern from an alite crystal along the [101] direction. Arrows indicate strong incommensurate modulations, while arrowheads mark additional weak features. (c) SAED pattern from (b) shown at a glancing incidence. Note that the reflection rows indicated with arrows go straight and parallel to b* while the rows marked with arrowheads follow a curved trajectory. (d) Schematic drawing, which represents a reciprocal lattice (simplified in one dimension) where the diffuse rods observed in (a), are drawn in gray color, while the basic structure reflections, which are elongated in the electron beam direction, are in black. The cutting of the Ewald sphere by the diffused rods will produce a spot in the SAED pattern. However, since the Ewald sphere curves as it goes away from the incident beam, it will cut the rods at different heights provoking a displacement of the observed spots with respect to the basic lattice reflections. This phenomenon, considering the Ewald sphere and the reciprocal lattice in three dimensions and the two dimensions of the SAED pattern, is responsible for the curvature of the odd reflection rows observed in (c).

In Fig. 1, the results of the synchrotron XRD are presented. Alite in clinkers from Plant 1 gave an apparent rhombohedral single peak at $2\theta \approx 50.3°$, and alite in clinkers from Plant 2 gave a monoclinic double peak. The apparent rhombohedral alite in both the ordinary clinker and the mineralised clinker from Plant 1 can be expected to be of lower symmetry. Looking at the chemical analysis in Ref. [1], Table 1, it is seen that the level of impurities is too low to stabilise the rhombohedral high temperature form. The monoclinic nature of the alite in the three samples from Plant 2 can be attributed to their high content of MgO (3.2–4.1 wt.%, Ref. [1]) since it has been shown that doping with MgO stabilises the monoclinic polymorphs [12]. The absence of any signs of a change in symmetry in the X-ray experiments is in agreement with Mascolo et al. [13], Mascolo and Ramachandran [14], and Kondo and Yoshida [15], who stated that the changing reactivity is not directly correlated with the crystal symmetry but rather to the chemical composition of the alite.

In order to further investigate the structural features of the alites from Plant 1, they were examined by transmission electron microscopy. The selected area ED (SAED) patterns recorded for alite in the ordinary and mineralised clinker turn out to be very similar, which again supports the notion that no change of polymorph has occurred. In Fig. 2, we show SAED patterns whose basic reflections (the more intense ones) have been indexed in the small monoclinic cell determined by Mumme [16] for an M_3 alite (space group Cm, $a = 12.35$, $b = 7.07$, $c = 9.30$ Å, and $\beta = 116.3°$). These basic intense reflections represent the basic alite structure without considering the tilting of the tetrahedra or other structural modulations.

The SAED pattern in Fig. 2a has been taken along the [010]-alite-orientation, which usually shows the presence of superlattice reflections in the literature (for example, see Ref. [11]. However, in this case, we cannot observe well-defined superlattice reflections but diffuse rods. In most of the cases, these rods apparently tend to condense into three spots (as in the case presented), but in some other cases, they are more uniform and diffuse. On the other hand, when the crystals are observed along the [101] direction (Fig. 2b), they do not show diffused rods but rather sharper and more intense incommensurate modulations marked with arrows. When incommensurate modulations appear, the reciprocal lattice can be described by the general expression $\boldsymbol{G} = \boldsymbol{H} \pm m\mathbf{q}$, where $\boldsymbol{G}$ represents any lattice point and $\boldsymbol{H}$ only the basic lattice; $\mathbf{q}$ is the vector that defines the modulation relating the satellite reflections with the basic lattice. The integer number m defines the order of the modulation harmonics. Thus, when $m = 0$, only the basic lattice reflections are defined. In the present case, the modulation vector $\mathbf{q} \approx 0.88\ \mathbf{a}^*$ and only the first harmonics can be observed, i.e., we see only values of $m = \pm 1$ indicating that the shape of the modulation wave is basically sinusoidal. In this SAED pattern, some other weak features are also present and are marked with arrowheads in the figures. If the diffraction pattern is observed at a glancing incidence along the [010]* direction (Fig. 2c), it is evident how the weak satellite rows bend towards the [10-1]* direction as we move away from the incident beam, i.e., for high k values, these weak satellites get closer to the upper basic $hk - h$ row than to the lower one. The reason is that the Ewald sphere is cutting the diffuse rods, which appear on the [010] zone axis. This zone axis is perpendicular to the [101] zone axis but the diffuse rods have an inclination angle. Due to the curvature of the Ewald sphere and depending on the distance from the incident beam, the Ewald sphere will cut the diffuse rods at different heights changing the reciprocal distance

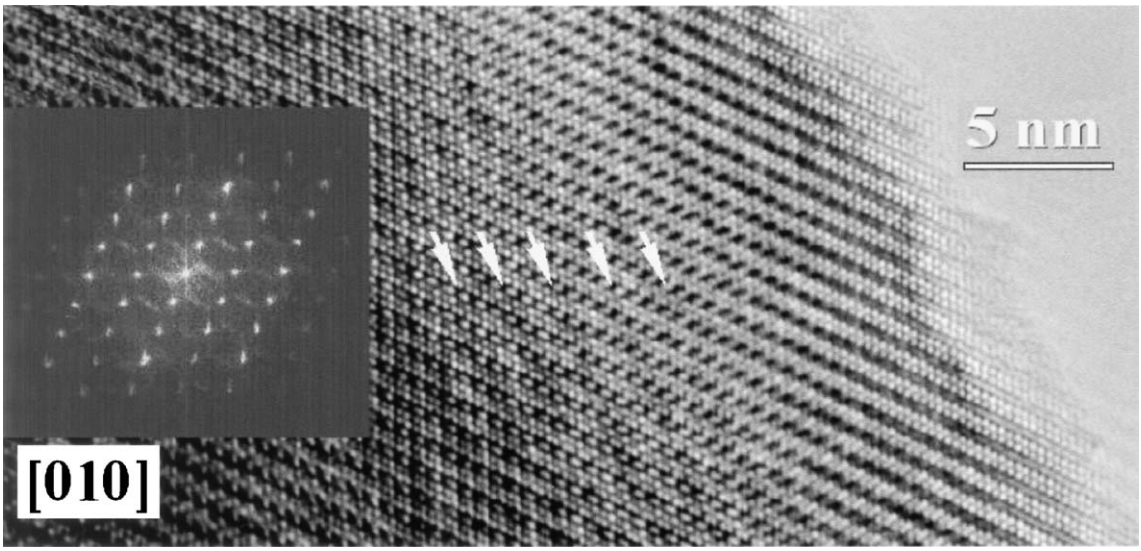

Fig. 3. HREM image of an alite crystal along the [010] direction. Inserted is the Fourier transform of the image. Notice how the diffuse rods are still present, and they correspond to the dark fringes marked with white arrows.

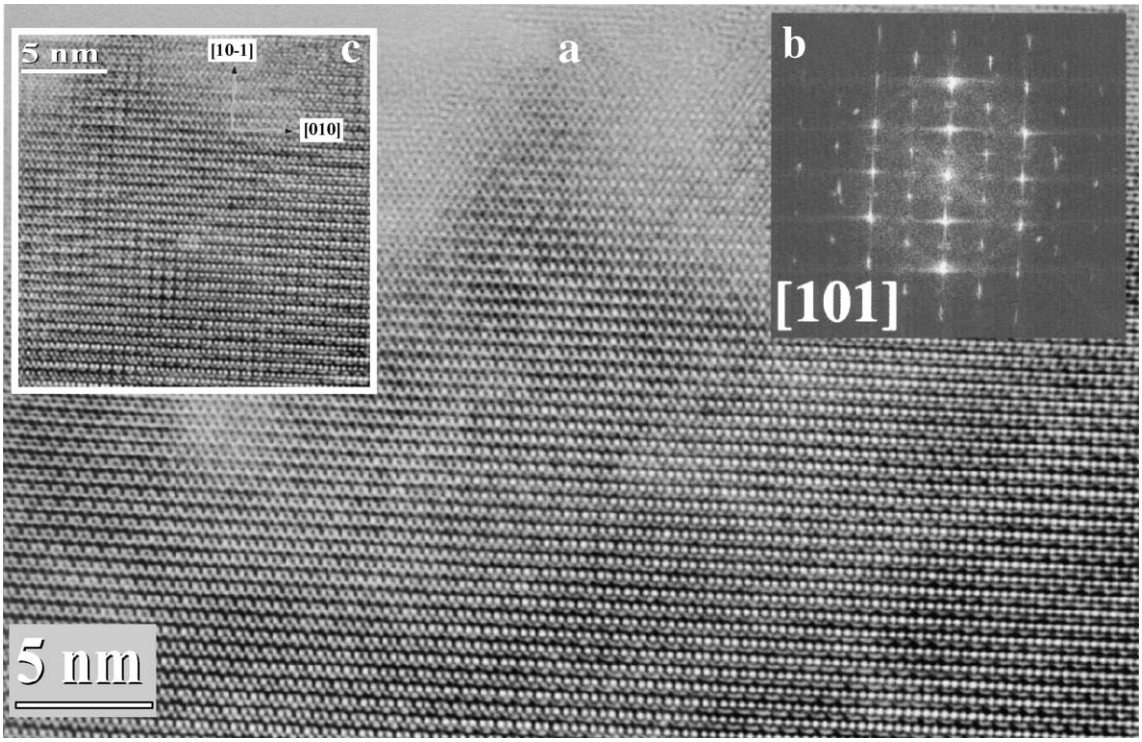

Fig. 4. (a) HREM micrograph from an alite crystal along the [101] direction. Inserted is the corresponding Fourier transform (b). Notice that although the satellites are still present, they are more diffuse and weak than in Fig. 2b due to radiation damage. In (c), the central part of the image has been processed increasing the satellites intensities three times with respect to the basic lattice reflections; thus, allowing the observation of the microdomains responsible of the incommensurate modulation.

between the $hk-h$ row and the weak satellites (see the scheme drawn in Fig. 2d).

In Fig. 3, we show a high-resolution electron microscopy (HREM) image of an alite crystal along [010]. In this image, dark fringes running almost parallel to the crystal edge are observed. The image Fourier transform inserted in the figure show diffuse lines, which correspond to the dark fringes observed in the image. However, when the images are taken along [101] (Fig. 4), the contrast due to the satellite reflections of the SAED pattern (Fig. 2b), disappear very quickly due to radiation damage. In the image shown in Fig. 4a, the contrast due to these satellites is still present although rather weak, as the Fourier transform of the image in Fig. 4b demonstrates. To be able to see the contrast in the real image that corresponds to the satellites, we have processed the image, increasing the satellites' intensity three times with respect to the basic structure reflections (see Fig. 4c). In the processed image, we can distinguish small domains ($\sim$5 nm in diameter) where the cell is doubled along [10-1], these small domains being in antiphase relationship with the neighboring microdomains.

These results suggest that the origin of the incommensurate modulation along the b^* direction has a different nature than the diffuse rods observed at the [010] zone axis. While the incommensurate modulation is very sensitive to radiation damage, the diffuse rods are very stable under the electron beam; and despite their diffuse nature in reciprocal space, they are easily observed in real space as dark fringes, which run without a very well-defined long-range orientation. The type of modulation observed in alite from Plant 1 has previously been shown to exist in production clinker from Buxton [17], as well as in Ti-doped alite and Al + F-doped Ca_3SiO_5 [11]. The exact relationship between the modulated structure observed here and the known polymorphs of alite and Ca_3SiO_5 remains to be determined, but this is beyond the

Table 2
Average microprobe analysis of belite, estimated S.D. (in parenthesis) referring to the last digit

Molar content	Plant 1		Plant 2		
	Ordinary	Mineralised	Ordinary	Mineralised (low SO_3)	Mineralised (high SO_3)
Ca	1.90(1)	1.89(3)	1.94(4)	1.96(3)	1.93(2)
Si	0.91(2)	0.87(5)	0.94(3)	0.94(3)	0.91(1)
Al	0.07(1)	0.08(3)	0.05(2)	0.04(2)	0.06(1)
Fe (3+)	0.037(4)	0.029(6)	0.019(6)	0.016(6)	0.022(3)
Mg	0.011(2)	0.011(6)	0.02(2)	0.01(1)	0.026(8)
S (6+)	0.021(4)	0.04(2)	0.008(5)	0.008(5)	0.020(7)
Ti	0.004(2)	0.005(2)	0.004(2)	0.001(1)	0.002(1)
P	0.01(1)	0.02(2)	0.01(1)	0.01(2)	0.008(7)
Na	0.026(6)	0.02(1)	0.03(1)	0.01(1)	0.026(4)
K	0.016(2)	0.012(4)	0.009(5)	0.005(2)	0.009(2)
O	4	4	4	4	4
No. of analyses	14	11	19	15	12

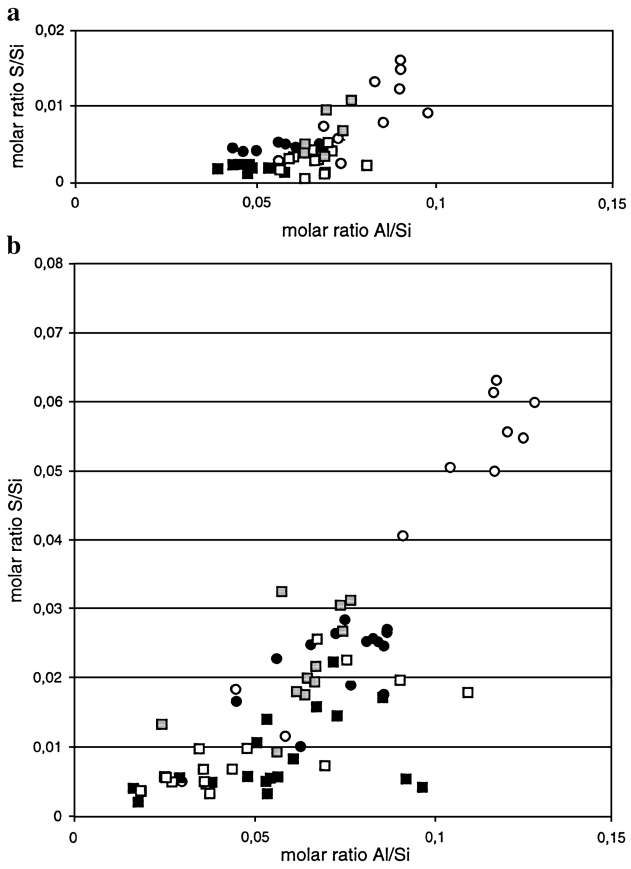

Fig. 5. Molar ratio Al/Si and S/Si in (a) alite and (b) belite (individual grains). Black circles are ordinary Portland clinker and white circles are mineralised clinker from Plant 1. Black squares are ordinary Portland clinker, white squares are low SO_3, and gray squares are high SO_3 mineralised clinker from Plant 2.

scope of the present investigation. Nevertheless, we conclude that the diffuse rods and satellite pairs definitely break the rhombohedral symmetry.

According to the second mechanism [3], the change in hydraulic activity can be explained by the introduction of defects with substitutions and solid solutions. Herfort et al. [18] suggested that the main solid solution in alite, in clinkers mineralised with calcium sulfate, and calcium fluoride is the substitution of S^{6+} and Al^{3+} for Si^{4+} in the tetrahedral sites: $3\ Si^{4+} \Longleftrightarrow S^{6+} + 2\ Al^{3+}$. To investigate the substitutions in the silicates, microprobe analysis was performed (Tables 1 and 2). The results all fall within the range of typical alite and belite compositions in ordinary Portland clinker [2], and the changes in the average composition caused by the mineralisation are indeed small. To study the individual results in detail, the molar sulfur to silicon ratios were plotted versus the molar aluminium to silicon ratios (see Fig. 5). Approximately 5% of the silicon sites in nonmineralised clinkers are occupied by aluminium, implying that the silicates incorporate some aluminium independently of the mineralisation and the presence of sulfur. It should also be noted that the level of substitution in belite is considerably higher than in alite.

As stated by Taylor [19] and Pollitt and Brown [20], the amount of SO_3 that enters the silicate phases depends on both the actual amount of SO_3 in the clinker and the molar SO_3 to alkali oxide ratio, R. If R is less than 0.8, most sulfur will combine with alkali to form calcium and alkali sulfates, and there will be little sulfur available for the silicates. In Fig. 6, the average amount of SO_3 in the two silicates is plotted versus R for the clinkers [1]. As expected, practically no SO_3 is incorporated in the silicates at $R < 0.8$. To achieve a maximum amount of SO_3 in the silicates, R must exceed 2. Both Plant 1 and 2 increased the SO_3 content in the mineralised clinkers [1]. However, the mineralised clinker of Plant 1 was the only clinker reaching $R>2$. This clinker consequently has also incorporated the largest amount of sulfur and aluminium in the alite and belite phases (see Figs. 5 and 6).

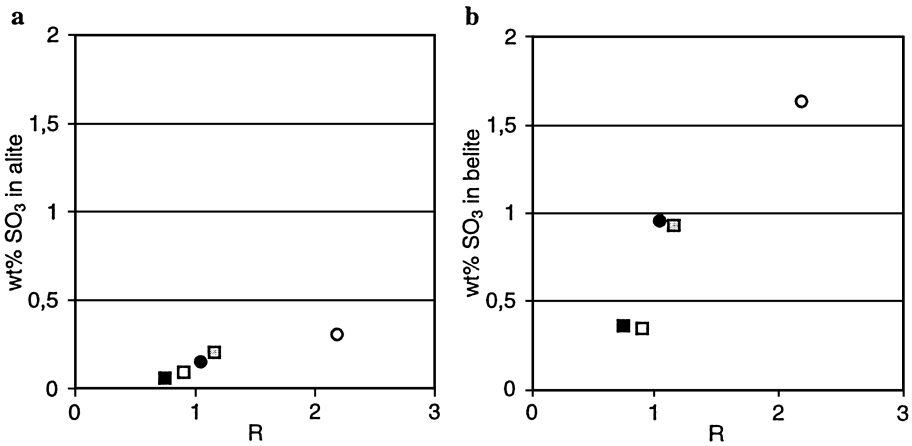

Fig. 6. The average amount of SO_3 in (a) alite and (b) belite plotted versus the molar SO_3 to alkali oxide ratio (R). Black circles are ordinary Portland clinker and white circles are mineralised clinker from Plant 1. Black squares are ordinary Portland clinker, white squares are low SO_3, and gray squares are high SO_3 mineralised clinkers from Plant 2.

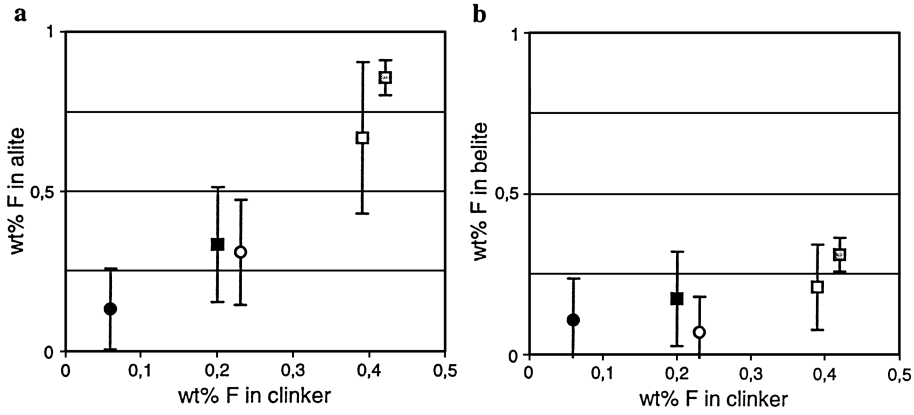

Fig. 7. The amount of F in (a) alite and (b) belite (average of 3-5 analyses, error bars represent ±1 estimated S.D.) plotted versus the amount of F in the clinker [1]. Black circles are ordinary Portland clinker and white circles are mineralised clinker from Plant 1. Black squares are ordinary Portland clinker, white squares are low SO_3, and gray squares are high SO_3 mineralised clinkers from Plant 2.

It has been suggested that the incorporation of aluminium can be coupled to the incorporation of fluorine [7] in oxygen sites according to the mechanism: $Si^{4+} + O^{2-} \Longleftrightarrow Al^{3+} + F^{-}$. It is hard to find a conventional method with sufficient sensitivity to study the fluorine content in the silicates. However, if the microprobe analysis of fluorine in the silicates is compared to the total amount of fluorine in the clinker, determined using an ion selective electrode [1], there are indications that the fluorine level is proportional to the total fluorine content of the clinker (see Fig. 7). It is also noted that fluorine is enriched in alite, i.e., the weight percent of fluorine is higher in alite than the average weight percent of fluorine in the clinker. Alite in the high SO_3 mineralised clinker from Plant 2 incorporated the largest amount of fluorine (0.86 wt.%) although the sulfur and aluminium level was not remarkably high. Alite in the mineralised clinker from Plant 1 had the highest sulfur and aluminium level but only incorporated 0.31 wt.% fluorine. Thus, there seems to be no correlation between the coupled sulfur/aluminium substitution and the incorporation of fluorine in alite. The two substitutions due to mineralisation should therefore be considered as separate phenomena.

According to the third mechanism suggested in Ref. [3], the retarding effect of fluoride can be attributed to the formation of barrier layers of insoluble CaF_2 on the surface of the clinker minerals. There is an optimum level of fluoride when mineralising clinker [3,9]. To reach maximum early strength (16–24 h), the fluoride content in the clinker should be ~0.2 wt.% as in the Plant 1 mineralised clinker [1]. The Plant 2 mineralised clinkers contain 0.4 wt.% fluoride, and thus exceed this level, which explains the retarded reaction rates of cements based on these clinkers.

4. Final remarks

It is concluded that the alite polymorph in the samples studied here is determined by the overall process and the raw mix rather than by the addition of fluoride and calcium sulfate as mineralisers. Alite in the Plant 1 clinkers is suggested to be pseudorhombohedral, with an incommensurate modulated structure. Alite in the Plant 2 clinkers is monoclinic. Belite is present in the monoclinic β-form in all clinkers. There are no indications in the present study that the polymorphism of alite or belite is changed due to the addition of the mineralisers.

The mineralising effect on the silicates is primarily related to the coupled substitution: $3\ Si^{4+} \leftrightarrow S^{6+} + 2\ Al^{3+}$. The molar SO_3 to alkali oxide ratio, R, should exceed 2 to get maximum substitution as in the Plant 1 mineralised clinker. Belite is often neglected when discussing mineralising effects although the level of aluminium and sulfur substitution is much higher than in the alite. Since the belite is a precursor of alite, it is possible that the substitutions in belite should be considered as an important factor for the reactivity of the silicates during the clinkering process. It may also affect the reaction rate of the hydrating cement primarily after about 12 h when belite starts to react. It should be noted that this coincides with the time for the accelerating hydration in the Plant 1 mineralised clinker. In this context, it is also of interest that the average size of the belite grains was smaller in the mineralised clinker from Plant 1 compared to the normal clinker [1], and thus possibly more reactive.

The decreased hydraulic activity of the mineralised clinkers from Plant 2 should be attributed to the high levels of fluoride, which might contribute to the formation of insoluble barrier layers on the surface of the clinker minerals during the hydration.

Acknowledgements

Cementa has supported this project financially. The authors would like to thank Hans Harryson, Department of Earth Sciences, Uppsala University for microprobe analysis

and Duncan Herfort, Aalborg Portland, as well as Erik Viggh and Sven-Erik Johansson, Cementa, for stimulating discussions.

References

[1] A. Emanuelson, S. Hansen, E. Viggh, A comparative study of ordinary and mineralised Portland cement clinker from two different production units: Part I. Composition and hydration of the clinkers, Cem. Concr. Res. 2003 (this issue).
[2] H.F.W. Taylor, Cement Chemistry, 2nd ed., Thomas Telford, London, 1997.
[3] G.K. Moir, F.P. Glasser, Mineralisers, modifiers and activators in the clinkering process, Proceedings of the 9th International Congress on the Chemistry of Cement, New Delhi, vol. 1, National Council for Cement and Building Materials, New Delhi, 1992, pp. 125–152.
[4] M. Regourd, Polymorphic transformations of tricalcium silicate, Rev. Mater. Constr. 620 (1967) 167–176.
[5] I. Maki, K. Kato, Phase identification of alite in Portland cement clinker, Cem. Concr. Res. 12 (1982) 93–100.
[6] M. Regourd, Détermination des réseaux de cristaux microscopiques. Application aux différentes formes du silicate tricalcique, Bull. Soc. Fr. Mineral. Cristallogr. 87 (1964) 241–272.
[7] H.E. Borgholm, D. Herfort, S. Rasmusen, A new blended cement based on mineralised clinker, World Cem. 8 (1995) 27–33.
[8] G.K. Moir, Improvements in the early strength properties of Portland cement, Philos. Trans. R. Soc. Lond., A 310 (1983) 127–138.
[9] G.K. Moir, Mineralised high alite cements, World Cem. 10 (1982) 374–382.
[10] E.G. Shame, F.P. Glasser, Stable Ca_3SiO_5 solid solutions containing fluorine and aluminium made between 1050 ° and 1250 °C, Br. Ceram., Trans. J. 86 (1987) 13–17.
[11] W. Sinclair, G.W. Groves, Transmission electron microscopy and X-ray diffraction of doped tricalcium silicate, J. Am. Ceram. Soc. 67 (1984) 325–330.
[12] R.T.H. Aldous, The hydraulic behaviour of rhombohedral alite, Cem. Concr. Res. 13 (1983) 89–96.
[13] G. Mascolo, B. Marchese, G. Frigione, R. Sersale, Influence of polymorphism and stabilizing ions on the strength of alite, J. Am. Ceram. Soc. 56 (1973) 222–223.
[14] G. Mascolo, V.S. Ramachandran, Hydration and strength characteristics of synthetic Al-, Mg- and Fe-alites, Matér. Constr. 8 (1975) 373–376.
[15] R. Kondo, K. Yoshida, Misciblities of special elements in tricalcium silicate and alite and the hydration properties of C_3S solid solutions, Proceedings of the 5th International Symposium on the Chemistry of Cement, Tokyo 1968, vol. 1, Cement Association of Japan, Tokyo, 1969, pp. 262–274.
[16] W.G. Mumme, Crystal structure of tricalcium silicate from a Portland cement clinker and its application to quantitative XRD analysis, N. Jb. Miner. Mh. 4 (1995) 145–160.
[17] K.E. Hudson, G.W. Groves, The structure of alite in Portland cement clinker-TEM evidence, Cem. Concr. Res. 12 (1982) 61–68.
[18] D. Herfort, J. Soerensen, E. Coulthard, Mineralogy of sulfate rich clinker and the potential for internal sulfate attack, World Cem. 5 (1997) 77–85.
[19] H.F.W. Taylor, Distribution of sulfate between phases in Portland cement clinkers, Cem. Concr. Res. 29 (1999) 1173–1179.
[20] H.W.W. Pollitt, A.W. Brown, The distribution of alkalis in Portland cement clinker, Proceedings of the 5th International Symposium on the Chemistry of Cement, Tokyo 1968, vol. 1, Cement Association of Japan, Tokyo, 1969, pp. 322–333.